

Frost salt scaling resistance of concrete containing CFBC fly ash

Michał A. Glinicki · Marek Zielinski

Received: 3 March 2008 / Accepted: 30 September 2008 / Published online: 11 October 2008
© RILEM 2008

Abstract The possibility for using coal combustion by-products in concrete exposed to frost-salt aggression was investigated. The research was aimed to assess an influence addition of circulating fluidized bed combustion (CFBC) fly ash on frost-salt scaling of air-entrained concrete. For evaluation of the resistance of concrete to frost salt scaling the test called “depth sensing indentation” (DSI) was applied. The DSI test method was implemented on a universal testing frame using a standard Vickers indenter. Experimental tests were performed on cement paste specimens and concrete specimens designed with partial replacement of cement with coal combustion by-products. The mass of scaled material in standard frost salt scaling resistance tests on concrete was inversely proportional to the Vickers hardness of the paste containing CFBC fly ash; the best-fit arithmetic relationship is provided.

Keywords Air entrained concrete · CFBC fly ash, Frost scaling resistance · Hardened cement paste · Microhardness

1 Introduction

The use of circulating fluidized bed combustion (CFBC) of coal for clean power production is rapidly growing in several countries [1, 2]. Such a coal combustion process is associated with the production of two types of by-products, i.e. CFBC bottom ash and CFBC fly ash, which differ in their particle size distribution, the content of unburned carbon and the chemical composition. Common components are, however, unreacted and reacted sorbent used for desulfurization, and unreacted coal/char. CFBC fly ash captured by electrostatic precipitators and having a particle size distribution within the range of approximately 1–300 μm , usually contributes a major part of the ash production, up to 70%. Mainly due to the presence of sorbent material and the lower combustion temperature (400–800°C less than the temperature in conventional boilers), the solid residue coming from coal combustion in fluidized bed boilers differs in its physical, chemical and mineralogical properties from the fly ash commonly used as a mineral additive in the concrete industry according to standards EN 450-1 [3] or ASTM C 618 [4]. Moreover, according to the European standard definition, fly ash is a fine powder of mainly spherical, glassy particles derived from burning the pulverized coal, with or without co-combustion materials. In case of CFBC fly ash, grains are non-spherical and the glassy phase is not present, so that CFBC fly ash is beyond its scope.

M. A. Glinicki (✉) · M. Zielinski
Institute of Fundamental Technological Research, Polish
Academy of Sciences, Swietokrzyska 21, 00-049 Warsaw,
Poland
e-mail: Michal.Glinicki@ippt.gov.pl

Several attempts to use fly ash from fluidized bed combustion as concrete additive were reported, e.g. [5–8]. Sebok et al. [6] found that the compressive strength of specimens containing fluidized bed combustion products depends on the mixing ratio of the compounds and the composition of binder. Test results indicated that the compressive strength after 2 years of hardening had a tendency to increase with increases of calcite and ettringite content in the specimens and to decrease with increasing contents of portlandite and gypsum. The compressive strength of concrete was found to increase as a result of partial replacement of cement by CFBC fly ash at the age of 7 days and this strength gain was stable under laboratory conditions, amounting to up to 39% after 2 years [7, 8]. However, the addition of CFBC fly ash resulted in a major decrease in slump of the concrete mix at a constant water to binder ratio. The recent study of microstructure of air voids in hardened air-entrained concrete [9] revealed the influence of CFBC fly ash on specific surface of air voids and the spacing factor. However, no data is available for the frost-salt scaling of concrete modified with addition of such non-standard coal combustion by-products. There is a strong sustainability-driven need to provide a basis for the development of an effective technology for the utilization of CFBC by-products in the concrete industry; in numerous countries the frost-salt aggression is a major durability concern for outdoor engineering structures.

The damage due to the combined action of frost and de-icing salts consists of the removal of small chips or flakes of material at the exposed surface of concrete; the phenomenon is called ‘frost salt scaling’ or simply ‘salt scaling’, or even ‘surface scaling’ to differentiate such damage from internal frost damage. Such surface damage is progressive and is known to depend on several technological factors, mainly on the water to cement ratio, the air entrainment, the cement content and the maturity of concrete, [10]. The majority of experimental data indicate that partial replacement of cement with standard fly ash or slag results in a marked increase of mass of scaled material. The frost salt scaling phenomenon has been studied thoroughly by numerous researchers and recently the research has been reviewed by Valenza and Scherer [11]. They also proposed a mechanical model showing that salt

scaling was a consequence of the fracture behavior of ice. The scaling can be enhanced when chloride salts are used due to an expansion resulting from precipitation of Friedel’s salt; the crystallization pressure from growth of these crystals causes significant expansion of the paste, and results in high stresses on a local scale near the ice/paste boundary. Theoretical considerations indicate that the strength of the concrete surface governs the ability of a cementitious body to resist frost salt scaling. However no attempt has been undertaken to define this ‘local’ strength more precisely. Pigeon, Marchand and Pleau [12] suggested that it was probably related to the microstructure of the very surface layer or ‘skin’ of concrete. Not very much is known about the microstructure of surface layers, however certain features can be expected. As shown in Fig. 1 surface layers of concrete are mostly composed of cement paste that tends to be more porous than that of bulk concrete. Since surface layers are often subjected to drying and wetting some extra microcracks can be induced and the pore size distribution of cement paste may be altered.

A proper test method to characterize the local strength of concrete in surface layers could be a microindentation test performed at a selected level of accuracy. The method based on the microhardness testing concept is well known for evaluation of the quality of engineering materials, particularly metals, and for over a decade has been attempted to be used for cement based materials [13–16]. The possibility of characterization of the microstructure and strength of cement paste by microhardness testing was discussed by Igarashi et al. [13]. The depth—sensing

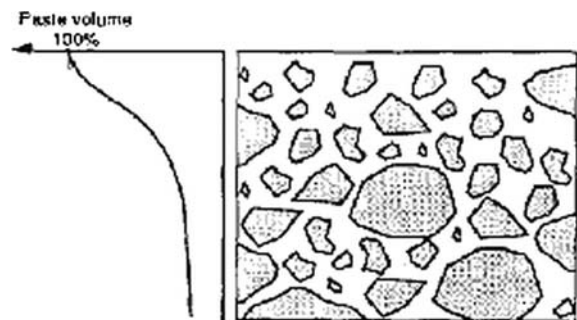


Fig. 1 Schematic description of paste content variability along the distance beneath the concrete surface (reproduced from [12])

microindentation technique was successfully used to study the elastic modulus and micro-strength of the interfacial transition zone around steel reinforcement in reinforced concrete [14]. Recently, the microindentation testing concept has been proposed for evaluation of the effectiveness of secondary cementitious materials [15] and in a more sophisticated test set-up, along with acoustic emission analysis, for identification of silica fume presence in hardened concrete [16]. The adequacy of microindentation testing for evaluation of the strength of concrete ‘skin’, has not been reported, except in [17]. It seems logical to seek a relationship between microindentation results and a concrete property such as the frost salt scaling resistance, that is supposed to depend on the near surface strength of a cementitious body. Such was the concept employed for the analysis of frost-scaling experimental data reported in this paper.

The objective of this investigation was to study the influence of two types of fly ash, coming from fluidized bed combustion boilers in selected power plants in Poland, on the frost salt scaling resistance of concrete. Experimental tests were performed on several concrete mixes designed with substitution of a part of cement by CFBC fly ash.

2 Experimental

2.1 Materials and specimens

Ordinary Portland cement CEM I 32.5 R (the chemical composition is given in Table 1), crushed basalt aggregates with grain sizes of 2–8 mm and 8–16 mm, sand with a maximum grain size of 2 mm, ordinary tap water, a high range water reducer based on a polycarboxylatether and air entraining admixture were used for concrete manufacturing. The following mineral additives were also used:

- CFBC fly ash from hard coal combustion in a power plant in Warszawa, Poland (FLW),
- CFBC fly ash from hard coal combustion in a power plant in Katowice, Poland (FLK).

Both types of CFBC fly ash were used in the investigation reported in [9]. The chemical properties of CFBC fly ashes, determined using standard European procedures, are given in Table 1. In CFBC fly ashes a high content of sulfuric anhydride, SO_3 , a

Table 1 Chemical composition of CEM I 32.5 R and CFBC fly ash (“FLW” and “FLK”)

Test parameters (% by mass)	Contents		
	CEM I 32.5R	FLW	FLK
SiO_2	20.38	34.36	47.46
Al_2O_3	5.4	20.82	23.29
CaO	63.04	12.22	7.48
SO_3	2.5	6.58	3.56
Cl^-	0.02	0.12	0.08
CaO free	0.84	1.79	0.35
MgO	1.74	4.02	3.10
Fe_2O_3	2.82	6.29	7.53
Loss on ignition	1.66	11.77	3.30
Unburned carbon content by TGA-DTA	–	3.9	0.3

high loss on ignition and an increased content of free CaO should be noted. Since some loss on ignition can be attributed to the presence of calcium carbonates in CFBC fly ash, an estimation of unburned carbon content was obtained using the TGA-DTA method in a helium/air atmosphere.

Concrete mixes were designed with constant water to binder ratio of 0.42, a constant slump of 30 ± 10 mm and the air content from 6% to 8%. The CFBC fly ash was used as a replacement of the cement by weight up to 40%. A reference concrete mix made of pure Portland cement (named “CEM I”) was also designed. To achieve the target slump and air content the required amount of chemical admixtures was established experimentally. The proportions of concrete mixes are given in Table 2.

Concrete specimens for frost scaling testing were cast in the cubical moulds ($100 \times 100 \times 100$ mm) commonly used for compressive strength testing. The concrete mixes were produced in a laboratory mixer and were consolidated by vibration (5–7 s on a vibrating table). After 24 h in moulds at $\text{RH} > 90\%$ and at the temperature $18\text{--}20^\circ\text{C}$ specimens were demoulded and cured in high humidity conditions ($\text{RH} > 90\%$) at the temperature of $18\text{--}20^\circ\text{C}$ until the age of 28 days. Companion cube specimens for compressive strength testing were also manufactured and cured at the same conditions.

Cement paste specimens were manufactured using Portland cement CEM I 32.5 R, tap water

Table 2 Concrete mix proportions

Mix	Type of additive	Content (kg/m ³)					HRWR (l/m ³)	AEA (l/m ³)	
		Cement	Additive	Sand	Basalt 2–8 mm	Basalt 8–16 mm			Water
CEM I	None	340	0	643	652	681	142	1.70	0.34
FLW20	FLW	271	68	640	649	678	141	2.03	1.36
FLW30		236	101	637	646	674	140	2.70	2.02
FLW40		202	135	637	646	674	140	3.37	2.70
FLK20	FLK	271	68	640	649	678	141	2.03	1.36
FLK30		236	101	637	646	674	140	2.70	2.02
FLK40		202	135	637	646	674	140	3.37	2.70

HRWR high range water reducer, AEA air entraining admixture

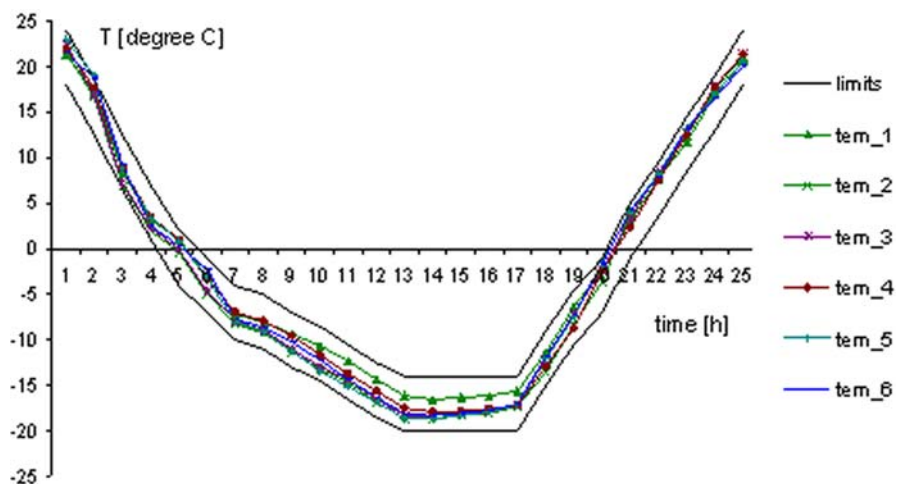
and two types of CFBC fly ash. A series of paste specimens with water to cement ratios of 0.40, 0.50 and 0.60 was prepared. In the second series the pastes were made with CFBC fly ash used as a partial replacement of cement by weight up to 35% and the water-to-binder ratio was constant at 0.42. Paste specimens for indentation testing were cast in 40 × 40 × 160 mm standard moulds. The curing regime was the same as for concrete specimens. At the age of 28 days a slice was cut from each beam using a diamond wheel saw and again stored in high humidity conditions (RH > 90%) at the temperature of 18–20°C. Before indentation testing, the specimen surface was polished with silicon powders (#320, #600 and #1200) to obtain a smooth surface such as used for microscopic investigation. At the initial stage of investigation flat specimens for indentation testing were also cut from manufactured concrete cubes.

2.2 Test procedures

2.2.1 Frost scaling

Frost scaling resistance of concrete was investigated according to the European standard procedure [18] that was established following the Swedish standard SS 137244 [19]. This laboratory method is in common use for determination of concrete resistance to repeated freezing and thawing (F/T) in contact with 3% sodium chloride (NaCl) solution. One freeze-thaw cycle requires 24 h and the limits for speed of temperature change are strictly defined (Fig. 2). After the specified number of cycles (usually 56 or 112), the amount of material scaled from the test surface, exposed to NaCl solution, was determined. Quantitative determination of the debris enables rating of frost scaling resistance of concrete. For instance: for concrete road pavements it is

Fig. 2 Temperature of salt solution at the concrete surface during frost scaling resistance test according to European standard



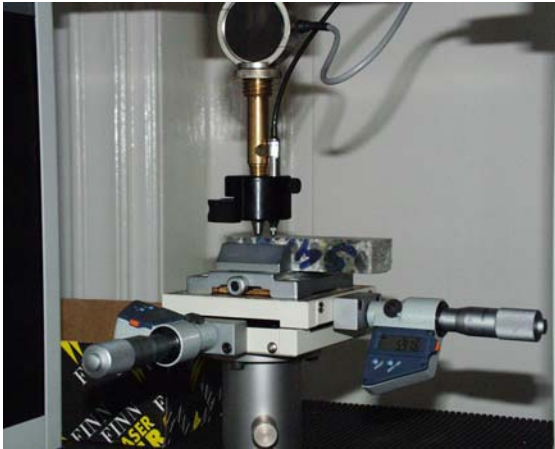


Fig. 3 Depth sensing indentation test set-up

common to assume the limit of allowable mass of scaled material as 1 kg/m^2 after 56 cycles.

2.2.2 Indentation

The depth sensing indentation (DSI) system involved pushing an indenter down into the specimen while measuring force and displacement continuously. Using a Lloyd EZ 50 testing machine suitably equipped for specimen holding (Fig. 3) the indentation load measurements were taken using a high precision load cell (the capacity of 50 N at the accuracy better than 0.5% of applied load). The LVDT transducer allowed a measurement of the displacement of indenter (h) into tested specimens with an accuracy of $0.1 \mu\text{m}$. The specimen holding fixture was installed on the movable stage with a manual movement control of an accuracy of 0.001 mm . A standard Vickers indenter was applied:

the indenter had the shape of a square-based pyramid. The measuring system and data acquisition were digitally controlled using Ondio-Nexygen software, which also enabled data post-processing.

The hardness value is defined as the ratio between the load and the contact area of the indentation in units of stress. Using measured values of load and displacement of indenter, the Vickers hardness (HV) can be calculated assuming a constant shape of indent due to the known geometry of the Vickers indenter:

$$HV = \frac{2P}{D^2} \sin \frac{\varphi}{2} = 1.854 \cdot \frac{P}{D^2} \quad (1)$$

where P = load (N), D = mean diagonal of indentation (mm) and φ is the angle between the opposite walls of the indenter.

Since the angle in the case of Vickers indenter $\varphi = 136^\circ$, the diagonal D is:

$$D \approx 7.001 \times h. \quad (2)$$

The DSI test was performed at the selected maximum load level of 40 N.

3 Test results and analysis

The average compressive strength of concrete cubes at the age of 28 days was 49.7 MPa for CEM I specimens. The average compressive strength of concrete containing CFBC fly ash was within the range from 54.3 to 56.4 MPa while the coefficient of variation was not higher than 6%. The partial replacement of cement by CFBC fly ash resulted in the compressive strength increase by few % at the age of 28 days.

Table 3 Mass of scaled material at the surface of concrete specimens exposed to 3% NaCl solution after freezing and thawing cycles (the exposed surface of $50,000 \text{ mm}^2$)

Concrete series	CFBC content (%)	Mass of scaled material (kg/m^2) after the number of F/T cycles			
		7	14	28	56
CEM I	0	0.006	0.016	0.036	0.090
FLW20	20	0.112	0.228	0.476	0.852
FLW30	30	0.096	0.290	0.564	1.210
FLW40	40	0.308	0.614	1.246	2.054
FLK20	20	0.040	0.112	0.250	0.516
FLK30	30	0.048	0.136	0.308	0.854
FLK40	40	0.206	0.388	0.876	1.524

Results of frost scaling resistance tests on concrete specimens are presented in Table 3. The mass of scaled material at the surface of concrete specimens was found to increase steadily with increasing number of freezing and thawing cycles. It was also found that increasing the cement replacement level resulted in a significant increase in the mass of scaled material. Such observations are consistent with generally reported experimental data for standard fly ash used as partial replacement of cement. Specific observations revealed quantitative differences in frost scaling resistance due to the type and quantity of CFBC fly ash used. Assuming a common criterion of acceptable frost scaling resistance of concrete as the mass of 1 kg/m^2 , certain concrete mixes could be classified as non-acceptable: FLW30, FLW40 and FLK40; the performance of FLK mixes was better.

To explain differences in frost scaling resistance of concrete the paste hardness data were used. An initial stage of investigation involved the DSI tests on polished specimens cut from manufactured concrete cubes. These attempts failed to provide comprehensive test results due to large inhomogeneity of material in relation to the size of Vickers indenter. At the load level of 40 N the diagonal of indentation was about 200–300 μm . Microscopic examination of indents at the specimen surface allowed only very few of them to be classified as pure paste indents; most of indentations affected paste and sand grains (or air voids) at the same time. Since the average distance between sand grains can be roughly estimated as about 200 μm it is evident that the precision of pointing the indenter into pure paste was not available.

An example of the load–displacement diagram obtained during testing of a cement paste specimen is presented in Fig. 4a. Points E1 and E2 indicate the beginning and the end of indenter travel in the tested material, respectively. The Vickers hardness values were determined on the basis of the measured load and the indenter displacement using the Eq. 1. At the selected load level it can actually be called the low-load hardness, using the accepted nomenclature. Each result of the DSI test was an average of 10 measurements made on the surface of the specimen. The scatter of results was low, i.e. the coefficient of variation was between 6% and 10%.

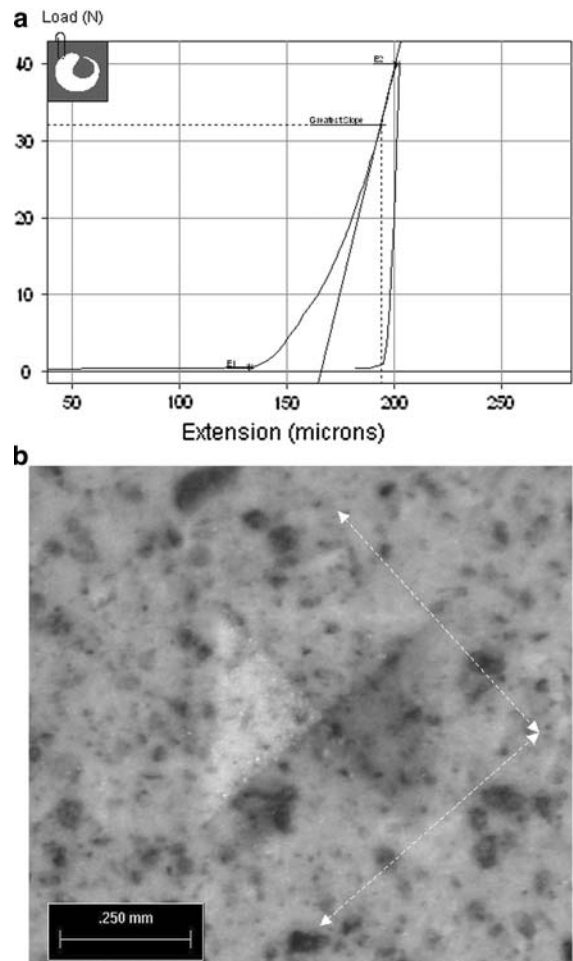


Fig. 4 Load versus indenter displacement diagram obtained during DSI testing on hardened cement paste and surface view of the indent in paste

Results of Vickers hardness measurements are presented in Figs. 5 and 6; each point represents the mean value of 10 measurements. A fairly linear relationship between water-to-binder ratio and Vickers hardness was found, where the binder mass is assumed as the sum of cement mass and CFBC fly ash mass. It is evident that Vickers hardness of cement paste decreased simultaneously with an increase of w/b ratio; its change from 0.40 to 0.60 relatively reduced HV by about 44–60%. It was also found that Vickers hardness significantly increased with age of specimens, roughly by 20–50% in relation to 28 day results. The maturity induced increase of Vickers hardness in absolute numbers was higher for lower w/b ratios. However, in relative terms the age effect was stronger for higher w/b.

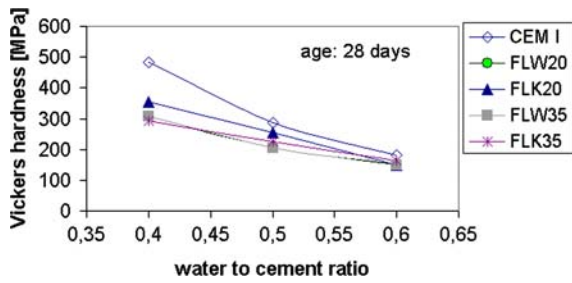


Fig. 5 Vickers hardness versus water-to-binder ratio for paste specimens containing CFBC fly ash at the age of 28 days (the average of 10 single tests)

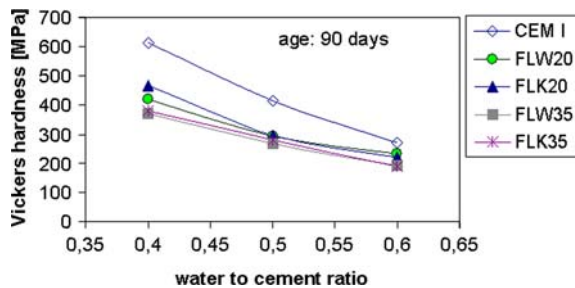


Fig. 6 Vickers hardness versus water-to-binder ratio for paste specimens containing CFBC fly ash at the age of 90 days (the average of 10 single tests)

The effect of cement replacement by CFBC fly ash was also evident: the hardness values decreased significantly with increasing replacement percentage, although such a decrease was significantly more pronounced for low w/b ratios. The applied cement replacement resulted in a relative decrease of HV down to about 60–70% of HV for pure Portland cement paste.

The experimental data on frost scaling resistance of concrete and the paste hardness are combined in Fig. 7 the Vickers hardness of cement paste of w/b = 0.40 at the age of 90 days and the mass of scaled material

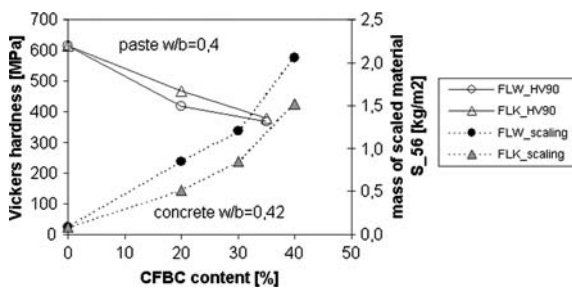


Fig. 7 The influence of CFBC fly ash content on Vickers hardness of cement paste at the age of 90 days and on the frost salt scaling of concrete specimens

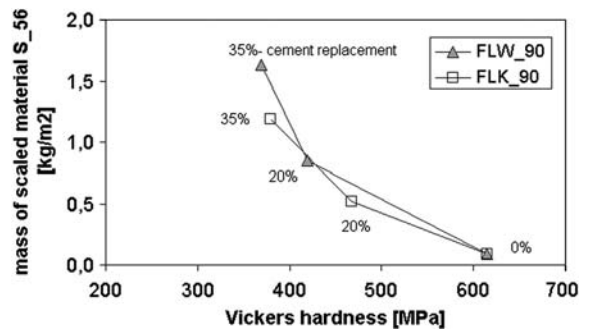


Fig. 8 The relationship between the Vickers hardness of cement paste at the age 90 days and the frost salt scaling of concrete containing CFBC fly ash

from concrete specimens of w/b = 0.42 are plotted at the applied cement replacement level.

It is clearly seen that the decrease of frost scaling resistance of concrete modified with CFBC fly ash addition can be associated with a decrease of Vickers hardness of cementitious paste. However such a relationship is expected to be influenced by other factors, such as the level of cement replacement and the type of additive. Surprisingly this was not the case. As shown in Fig. 8, plotting the frost scaling data versus the Vickers hardness data resulted in a unique relationship independent of the type and the quantity of additive used.

The regression analysis revealed the best fit ($R^2 = 0.997$) of the following formula:

$$S_{56} = 103.79 \exp(-0.0115 HV), \tag{3}$$

in which S_{56} —denotes the mass of scaled material after 56 cycles in the standard test expressed in kg/m^2 , HV—denotes the Vickers hardness of cement paste (with addition of CFBC fly ash) at the age of 90 days, expressed in MPa. Rearranging this formula one can estimate the Vickers hardness of cement paste required for a designed performance of concrete subjected to freeze-thaw and de-icing salt (3% NaCl) action.

4 Discussion

The significance of the established S_{56} –HV relationship should be discussed at least in respect to the following factors:

- the meaning of DSI test results for paste specimens for variable w/b ratio, age and content of CFBC additions,



- the adequacy of explanation of concrete frost scaling data using test data on paste specimens manufactured at somewhat different w/b ratio,
- the significance of air void system in concrete.

The effect of water-to-cement ratio on microhardness of cement paste has been noticed previously, e.g. in [13] and [20]; it has been correlated with the compressive strength of paste. Thus, the age induced effect on microhardness can be explained similarly to the age effect on compressive strength of the paste and can be attributed to the increasing degree of hydration of cement. This investigation was, however, performed at the load range corresponding to “low load hardness” at which some indentation size effect can be expected [21]. Thus, while the obtained HV values have a relative significance, no comparison of absolute values can be given. The major reason to select such a load range was the intention to perform indentation to a representative depth and to affect the volume of the material at a representative scale: the term “representative” has been assumed to have a specific meaning limited to the targeted phenomenon of frost scaling. Instead of the troublesome identification of the actually affected phase in cement paste using very low indentation loads, the assumed approach was aimed at obtaining an average mechanical characterization of a local region, including a whole range of hydration product sizes, microporosity, microcracks, microdefects and local inhomogeneities. The proportional decrease of HV with cement replacement using CFBC fly ash is considered representative for the “local” strength decrease. The best-fit empirical relationship is linear with respect to w/b ratio, e.g. for CEM I specimens it is: $HV = 0.67 (1/(w/b) - 1)$, while for FLK35 specimens it is: $HV = 0.60 (1/(w/b) - 0.80)$. A drop of HV accompanying an increase of CFBC fly ash content is not consistent with obtained results of concrete compressive strength manifesting the opposite trend. The available data [8, 22] on the compressive strength of concrete containing CFBC fly ash also show the tendency to increase the strength for increasing CFBC fly ash content while the workability of the mix is maintained with the use of water-reducing admixtures. Possible effects of CFBC fly ash on properties of interfacial transition zones deserve a detailed investigation.

According to [23] the excessive cement replacement by conventional fly ash retards the initial set time and the amount of bleeding increases with an increase in fly ash substitution. Current investigation did not include bleeding observations. However, the established correlation between S_{56} (concrete) and HV (paste) rather diminishes a possible influence of bleeding phenomenon. The obvious difference was in the w/b ratio in the concrete mix (0.42) and in the paste mix (0.40). Using HV data established for a range of w/b ratios in the paste one could interpolate HV for w/b = 0.42. This approach was abandoned, however, considering a local variation of w/b commonly expected in concrete. Thin section based investigations, described in [24], revealed a high variation of w/b dependent on the proximity of aggregate grains. Since a part of mixing water is needed to wet aggregate surfaces, the local w/b ratio around aggregates should be higher and this is commonly considered characteristic for the transition zone. Therefore the bulk paste should be characterized by slightly lower w/b ratio and in the current case w/b = 0.40 is assumed as a fair approximation. The passage from cement paste properties to properties of concrete is not straightforward because of several factors, including different homogeneity of grain dispersion due to mixing and different types of porosity of paste, associated with microcracks and discontinuities related to dimensional changes occurring during curing. Several developed models to predict permeability of concrete from the pore structure are known to have a common form of exponential relationship between permeability and some characteristic pore dimension, [25]. If one assumes that HV determination in the range of “low load hardness” is a homogenisation approach at a scale representative for paste porosity, the exponential form of the S_{56} –HV relationship is not astonishing. In spite of the limitations mentioned above, the practical use of such a relationship can reduce testing efforts needed to prove frost scaling performance of concrete containing CFBC fly ash.

The established S_{56} –HV relationship (Eq. 3) is consistent with the glue-spall model [11] that accounts for the major influence of strength of the surface on the ability of the cementitious body to resist frost salt scaling, provided that the surface strength can be directly associated with HV values determined using DSI. Tremblay et al. [17] also used

the concept of hardness testing to evaluate the strength of surface and to verify the glue-spall model. The indentation hardness was experimentally determined on mortar specimens using Brinell hardness test with a 500-kg load and revealed the same tendency for the surface hardness and the compressive strength to decrease with the presence of entrained air and with increase of water–cement ratio. The principal difference of the approach [17] and the current investigation is due to the load level difference by two orders of magnitude, implying the difference of the indent size by at least one order of magnitude. Such a large scale indentation obviously accounts for air voids and sand grains and has some other meaning than the current approach at a paste scale, considered as representative for paste porosity (excluding entrained air voids).

The observed increase of mass of scaled material for decreasing clinker content in concrete is consistent with published data on blended cement performance in frost scaling resistance tests [23, 26]. It should be noted that the mix design for the reference concrete (CEM I) was performed according to EN 206-1 standard prescriptive recommendations (XF4 exposure): minimum cement content 340 kg/m³, water-to-cement ratio ≤ 0.45 , air entrainment, adequate frost resistance of aggregates. As documented in [8] in Table 3 the conditions of adequate entrained air void system in hardened concrete (with and without addition of CFBC fly ash) were also met: the total air content from 5.26% to 7.08%, the spacing factor from 0.13 to 0.23 mm. The air void system in CFBC fly ash concrete was characterized by larger diameter of voids and increased spacing factor than in reference concrete, but still the differences were small and not sufficient alone to justify large differences in frost salt scaling resistance. The observed corruption of the air void system could be linked to the increased frost scaling degradation of CFBC fly ash concrete that was primarily influenced by a decrease of the surface microhardness. This observation confirms the significance of both the surface strength and the air void system in concrete in regard to frost salt scaling resistance but the balance between two effects is in contrast to the conclusions of recent work by Tremblay et al. [17] indicating that the reduced compressive strength and surface hardness has much less influence on the frost salt scaling than the beneficial effect of air entrainment. Thus the

effects induced by the use of non-standard additives to concrete as CFBC fly ash can not be quantitatively predicted using the already established knowledge.

5 Conclusions

The investigation revealed the following conclusions.

1. The use of CFBC fly ash in air entrained concrete resulted in a degradation of frost salt scaling resistance; the effect was pronounced for increasing cement replacement level and for increasing unburned carbon content of CFBC fly ash.
2. The mass of scaled material in standard frost scaling resistance tests on concrete was inversely proportional to Vickers hardness of cement paste; the obtained exponential-form relationship was independent of the type and the quantity of CFBC additive used.
3. The DSI test data provided the best fit empirical relationships between Vickers hardness of paste and the inverse of w/b ratio that was close to linear provided that the binder mass was assumed as the sum of cement mass and CFBC fly ash mass. A proportional decrease of HV with increasing content of CFBC fly ash was revealed.

Acknowledgement The investigation was financially supported by public funds for scientific research available for the period 2006–2009 (Polish Ministry of Science and Higher Education : Research Project no 4 T07E 036 30).

References

1. Basu P (1999) Combustion of coal in circulating fluidized-bed boilers: a review. *Chem Eng Sci* 54:5547–5557. doi: [10.1016/S0009-2509\(99\)00285-7](https://doi.org/10.1016/S0009-2509(99)00285-7)
2. Nowak W (2003) Clean coal fluidized-bed technology in Poland. *Appl Energy* 74:405–413. doi:[10.1016/S0306-2619\(02\)00195-2](https://doi.org/10.1016/S0306-2619(02)00195-2)
3. EN 450-1:2005 Fly ash for concrete. Definition, specifications and conformity criteria
4. ASTM C 618-03 Coal fly ash and raw or calcined natural pozzolan for use in concrete
5. Brandstetr J, Havlica J, Odler I (1997) Properties and use of solid residue from fluidized bed coal combustion. In: Chandra S (ed) *Waste materials used in concrete manufacturing*. Noyes Publications Press, Westwood, New Jersey, USA, pp 1–47
6. Sebok T, Simonik J, Kulisek K (2001) The compressive strength of samples containing fly ash with high content of

- calcium sulphate and calcium oxide. *Cement Concr Res* 31:1101–1107. doi:[10.1016/S0008-8846\(01\)00506-3](https://doi.org/10.1016/S0008-8846(01)00506-3)
7. Glinicki MA, Kobylecki R, Nowak W, Maslanka J (2004) Applications of mechanically activated ashes from fluidized bed coal combustion in Poland, 8th CANMET/ACI international conference on fly ash, silica fume, slag and natural pozzolans in concrete. In Proceedings of technical papers organized by The U.S. Advisory Committee, EPRI, Palo Alto, CA (CD-ROM)
 8. Glinicki MA, Nowowiejski G (2008) Long term strength of concrete with addition of fly ash from fluidized bed combustion of hard coal. Proceedings of 5th conference DNI BETONU 2008. Polish Cement Association, Wisla, Poland (in Polish)
 9. Glinicki MA, Zielinski M (2008) Air void system in concrete containing circulating fluidized bed combustion fly ash. *Mater Struct* 41:681–687. doi:[10.1617/s11527-007-9273-6](https://doi.org/10.1617/s11527-007-9273-6)
 10. Stark DC, Kosmatka SH, Farny JA, Tennis PD (2001) Performance of concrete specimens in the PCA outdoor test facility. RD124, Portland Cement Association, Skokie, Illinois, USA
 11. Valenza JJII, Scherer GW (2006) Mechanism for salt scaling. *J Am Ceram Soc* 89(4):1161–1179. doi:[10.1111/j.1551-2916.2006.00913.x](https://doi.org/10.1111/j.1551-2916.2006.00913.x)
 12. Pigeon M, Marchand J, Pleau R (1996) Frost resistant concrete. *Construct Build Mater* 10(5):339–348. doi:[10.1016/0950-0618\(95\)00067-4](https://doi.org/10.1016/0950-0618(95)00067-4)
 13. Igarashi S, Bentur A, Mindess S (1996) Characterization of the microstructure and strength of cement paste by microhardness testing. *Adv Cement Res* 30:87–92
 14. Zhu W, Bartos PJM (2000) Application of depth-sensing microindentation testing to study of interfacial transition zone in reinforced concrete. *Cement Concr Res* 30:1299–1304. doi:[10.1016/S0008-8846\(00\)00322-7](https://doi.org/10.1016/S0008-8846(00)00322-7)
 15. Glinicki MA, Zielinski M (2004) Depth-sensing indentation method for evaluation of effectiveness of secondary cementitious materials. *Cement Concr Res* 34:721–724. doi:[10.1016/j.cemconres.2003.10.014](https://doi.org/10.1016/j.cemconres.2003.10.014)
 16. Kasperkiewicz J (2006) On a possibility of structure identification by microindentation and acoustic emission. In: Bartos PJM (ed) Nanotechnology in construction. RI-LEM Proceedings pro045, pp 151–159
 17. Tremblay M-H, Lory F, Marchand J, Scherer GW, Valenza JJ (2007) Ability of the glue spall model to account for the De-Icer salt scaling deterioration of concrete. In: Beaudoin JJ, Makar JM, Raki L (eds) Paper W4-07.3 in proceedings of 12th ICCI. National Research Council of Canada, Montreal, Canada
 18. CEN/TS 12390-9 (2006) Testing hardened concrete—Part 9: freeze-thaw resistance—scaling. European Committee for Standardization, Brussels
 19. SS 137244 (1995) Concrete testing—hardened concrete—scaling at freezing
 20. Trtik P, Bartos PJM (1999) Micromechanical properties of cementitious composites. *Mater Struct* 32:388–393. doi:[10.1007/BF02479632](https://doi.org/10.1007/BF02479632)
 21. Igarashi S, Bentur A, Mindess S (1996) Microhardness testing of cementitious materials. *Adv Cement Base Mater* 4:48–57
 22. Zielinski M (2007) Influence of fluidized bed combustion fly ash on selected properties of mortar and concrete. *DROGI i MOSTY* No. 2: 59–85 (in Polish)
 23. Neuwald A, Krishnan A, Weiss J, Olek J, Nantung TE (2003) Concrete curing and its relationship to measured scaling in concrete containing fly ash. Transportation Research Board. Available at: http://cobweb.ecn.purdue.edu/~concrete/weiss/publications/r_conference/RC-019.pdf. Cited 5 Nov 2007
 24. Elsen J et al (1995) Determination of the w/c ratio of hardened cement paste and concrete samples on thin sections using automated image analysis techniques. *Cement Concr Res* 25(4):827–834. doi:[10.1016/0008-8846\(95\)00073-L](https://doi.org/10.1016/0008-8846(95)00073-L)
 25. Brown PW, Shi D, Skalny J (1991) Porosity/permeability relationships. In: Skalny J, Mindess S (eds) *Materials science of concrete II*. American Ceramic Society, Westerville, pp 83–109
 26. Bilodeau A, Malhotra VM (1992) Concrete incorporating high volumes of ASTM class F fly ashes: mechanical properties and resistance to de-icing salt scaling and to chloride-ion penetration. In: Malhotra VM (ed) *Fly ash, silica fume, and natural pozzolans in concrete*, proceedings of fourth international conference. ACI Special Publication SP-132, American Concrete Institute, Detroit, pp 319–349